



Article

Research on Electromagnetic-Radiated Emission of Multi-in-One Electric Drive System

Ruoxi Tan *, Shangbin Ye, Cheng Yu, Chenghao Deng and Anjian Zhou

Chongqing Changan New Energy Automobile Technology Co., Ltd., Chongqing 400023, China; ysb1990712@163.com (S.Y.); yucheng@changan.com.cn (C.Y.); dengch@changan.com.cn (C.D.); zhouaj@changan.com.cn (A.Z.)

* Correspondence: rxt_923@163.com; Tel.: +86-023-6315-6400

Abstract: The strong electromagnetic interference produced by the electric drive system is the main factor that leads to the strong radiated emission of electric vehicles. It is very important to study the influence of the electric drive system on vehicle-radiated emission by taking the common-mode current of the electric drive system as the interference source. In this paper, the conducted emission model of the electric drive system is proposed, and the common-mode current is calculated by this model. The influence of filter on the common-mode interference current of HVDC cables is calculated and analyzed, and then the radiating antenna effect model of HVDC cables is established. Based on this, a vehicle-level radiated emission simulation model including an electric drive system and DC cables was established. The effectiveness of the conducted emission model was verified by experiments. The effects of different shielding structures on the shielding efficiency of HVDC cables were compared. Quantitative guidance for EMI suppression design of multi-in-one electric drive system design can be provided by the model in this paper.



Citation: Tan, R.; Ye, S.; Yu, C.; Deng, C.; Zhou, A. Research on Electromagnetic-Radiated Emission of Multi-in-One Electric Drive System. *World Electr. Veh. J.* **2021**, *12*, 127. <https://doi.org/10.3390/wevj12030127>

Academic Editor: Hui Yang

Received: 17 July 2021

Accepted: 13 August 2021

Published: 21 August 2021

Publisher's Note: MDPI stays neutral with regard to jurisdictional claims in published maps and institutional affiliations.



Copyright: © 2021 by the authors. Licensee MDPI, Basel, Switzerland. This article is an open access article distributed under the terms and conditions of the Creative Commons Attribution (CC BY) license (<https://creativecommons.org/licenses/by/4.0/>).

Keywords: radiated emission; electric drive system; shielding cable; EMI; suppression

1. Introduction

As the power source of electric vehicles, the electromagnetic emission of the electric drive system is a great challenge to the EMC (electromagnetic compatibility, EMC) of electric vehicles. With the development of technology, the electric drive system gradually tends to be integrated and miniaturized, and more compact functional integration in limited space will undoubtedly make the problem of electromagnetic interference more serious. Therefore, aiming at the latest multi-in-one electric drive system composed of a motor controller, permanent magnet synchronous motor, reducer, and charger, the electric drive system used in electric vehicles has been considered as a noise source of both conducted and radiated electromagnetic interference due to its high du/dt (rate of change of voltage per unit time, du/dt) and di/dt (rate of current change per unit time, di/dt) of switching characteristics. The radiation of electric drive systems has been researched by many experts. The hybrid simulation technology of the moment method and transmission line method is used to analyze the impedance and radiation EMI (electromagnetic interference, EMI) of the cable of the electric drive system [1–3]. Aiming at the EMC problem of the motor drive system and its interference mechanism, an electromagnetic model construction simulation method for the study of the electromagnetic radiation intensity distribution in electric vehicles was also proposed [4,5]. Theoretical calculation and measurement of shielded cable transfer impedance for evaluation of cable shielding effectiveness is proposed by E.F.Vance, and theoretical models of tubular, braided, helically wound, and multi-layer shielded cables is introduced in detail [6]. Since then, many foreign experts and scholars, such as Tyni [7], Kley [8], Demoulin [9], S.Sali [10], etc., have improved the theoretical calculation model of transfer impedance of the Vance shielded cable. These theoretical derivations mainly focus on braided shielded cables. The contribution of the

flux connection between braided layers to the transfer impedance is further studied, and the theoretical calculation of the transfer impedance is gradually improved.

However, very little research of radiation interference modeling is based on the calculated conducted noise emission model of the electric drive system. The influence of shielding cable is also rarely considered in RE (radiated emission, RE) simulation.

In this paper, a radiated emission simulation model of a multi-in-one electric drive system is analyzed. The paper is organized as follows. A conducted emission simulation model of a MEDS (multi-in-one electric drive system, MEDS) is established in Section 2, and the common-mode current as the interference source is calculated by this model. The radiated emission model and the typical EMI suppression methods of EV (electric vehicle, EV) are described and analyzed in Section 3. The accuracy of the CE (conducted emission, CE) model of the MEDS is verified by comparing the tested data with the simulation data in Section 4, and the reliability of using the common-mode current as the interference source of the EV-radiated emission model is also indirectly proved. Then, the transfer impedance of the two kinds of shielded cables is compared and analyzed by simulation, and the effects of typical interference suppression methods on radiated emission are compared and analyzed on the vehicle model. Finally, a summary of major conclusions, the innovation and the limitations, and further proposed research is presented in Section 5.

2. Modeling of Conducted Noise of MEDS

The radiated model in this paper is based on the common-mode current calculation of the system-level conducted emission co-simulation model of MEDS [11]. The conducted emission model is shown in Figure 1. The IGBT (Insulated Gate Bipolar Transistor, IGBT) module is the fundamental cause of periodic di/dt and du/dt changes. Therefore, an equivalent circuit model of nonlinear dynamic switching characteristics of IGBT is established. The impedance and parasitic parameters of the filter and the PMSM (Permanent Magnet Synchronous Machine, PMSM), which provide a high-frequency coupling path for conducted noise, are described by an accurate impedance equivalent model. Structure parameters of DC cable module, AC (Alternating current, AC) copper bar module, and near-field coupling, are extracted as RLC (resistance, inductance, capacitance, RLC) parameters by 3D finite element simulation. Based on SIMULINK software, the equivalent model of the driver signal of the MEDS is established, as shown by the MATLAB icon in Figure 1. By integration of models above into a circuit model, the prediction model of conducted interference simulation platform of the MEDS is established.

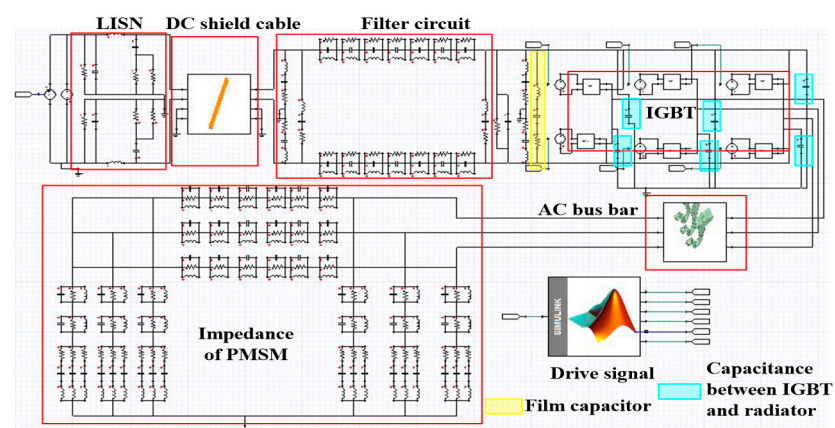


Figure 1. Conducted EMI emission simulation model of motor drive system.

The modeling method of conducted emission of the MEDS and the accuracy of the model are verified [11]. However, the radiated emission of the MEDS and the influence of shielding cable on the radiated emission of the system are not considered. Therefore, based on the conducted emission model, the common-mode current on the HVDC (high-

voltage direct current, HVDC) cable is calculated and as the interference source of radiated emission of the MEDS in the vehicle.

3. Radiated Emission Modeling and Interference Suppression

3.1. Radiated Emission Modeling

The common-mode current extracted from the HVDC cable port of the MEDS was taken as the interference source, and the HVDC cable model was taken as the radiation antenna on the propagation path and imported into the vehicle model. Based on the models above, a vehicle-level radiated emission model integrating the interference source and interference propagation path was established, as shown in Figure 2.

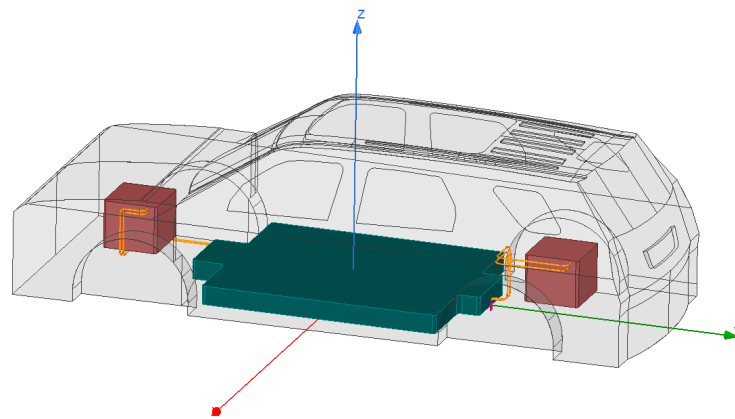


Figure 2. The EV model with two MEDS.

Considering the strong electromagnetic interference of the MEDS, the conductive emission interference of the MEDS needs to be suppressed. In this paper, the following methods are analyzed for interference suppression. Firstly, it is suggested to optimize the design of the filter on the HVDC cable. Secondly, the shielding efficiency of the HVDC cable is optimized to reduce the antenna radiation effect of the cable. The suppression effects of the two typical EMI suppression methods are calculated in the following section.

3.2. Analysis of Typical Vehicle EMI Suppression Methods

3.2.1. Interference Suppression by Filter Circuit

In order to suppress the interference on the HVDC cable, a π -type filter is added at the port. The complete π -type filter circuit model considering the high-frequency parasitic effect is shown in Figure 3.

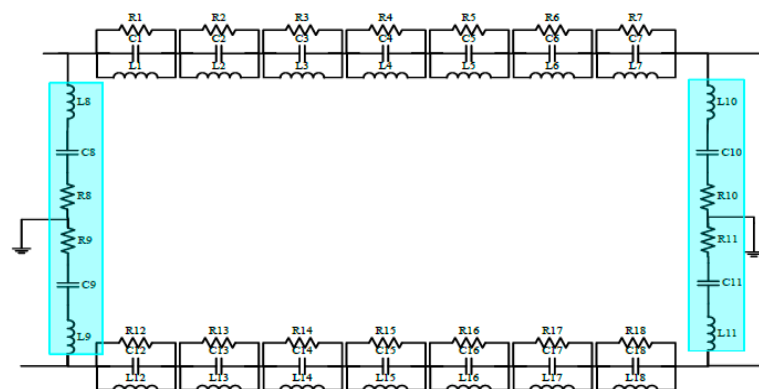


Figure 3. High-frequency equivalent model of π -type filter circuit.

By comparing the ports of the electric drive system with and without a high-frequency filter circuit, the calculated common-mode interference current (I_{cm}) of the electric drive

system is shown in Figure 4. It is shown that after adding the high-frequency filter circuit, the I_{cm} (blue curve) on the HVDC cable of the MEDS is significantly lower. As common-mode interference current is the main source of radiated emission at high frequency; the radiated emission of MEDS with filter circuit will also be reduced.

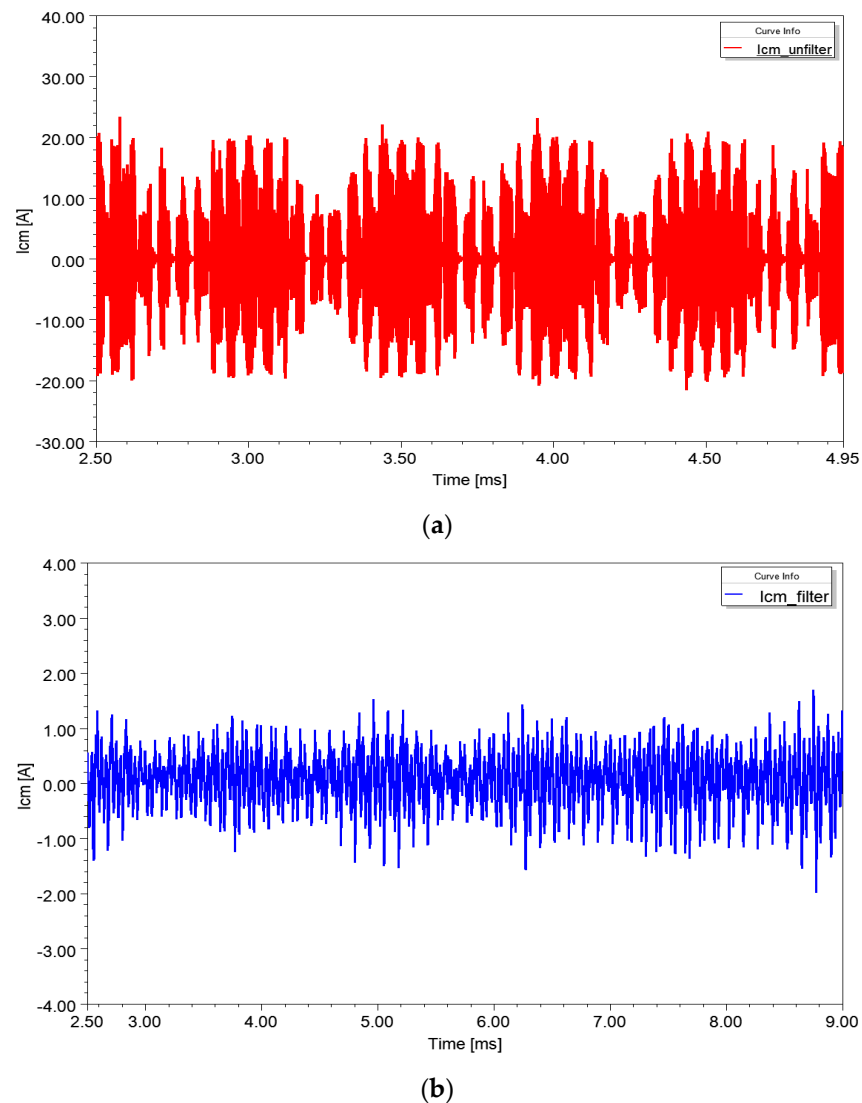


Figure 4. The common mode current: (a) without filtering; (b) with filtering circuit.

3.2.2. Interference Suppression for Shielded Cables

The HVDC shielding cable is used to transmit the energy of the battery pack to the power inverter and the three-phase AC drive motor, and it is crucial in the electric drive system model. Surface transfer impedance is an important parameter to describe the shielding efficiency of a high-voltage connection system. The smaller the transfer impedance is, the better the shielding performance of the shielded cable will be. The 3D electromagnetic modeling of transfer impedance for HVDC shielded cable is carried out based on high-frequency full-wave electromagnetic simulation software, as is shown in Figure 5. Cross-sections of three different cable models established based on finite element simulation software are shown in Figure 6; the finite element calculation is carried out by commercial software HFSS on the high-voltage shielding cable, and the transfer impedance value of each frequency band is obtained to evaluate the shielding effectiveness of the cable.

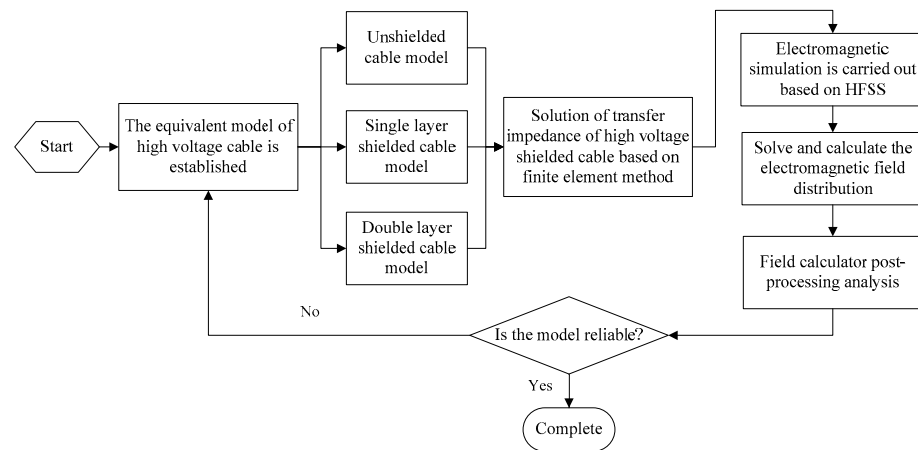


Figure 5. Modeling methods for high voltage without shielded and shielded cables.

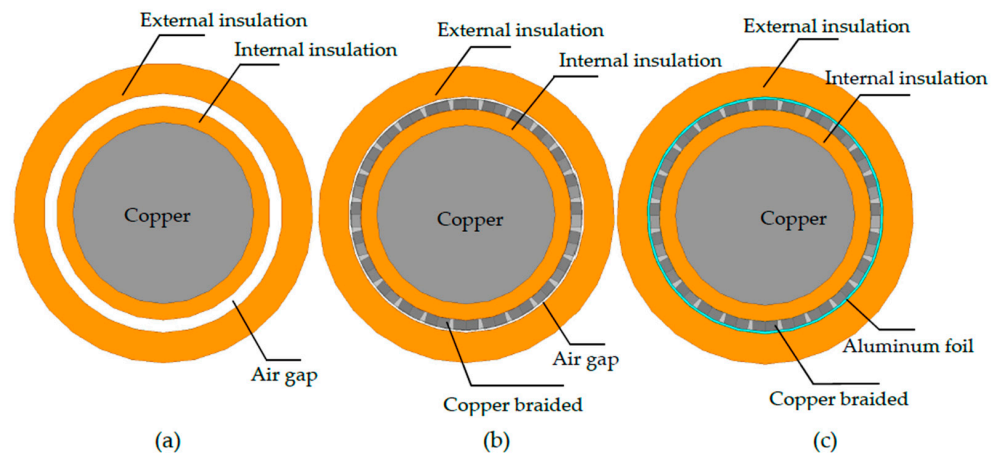


Figure 6. Cross sections: (a) unshielded cable; (b) single-shield cable; (c) double-shield cable.

Because the plane wave excitation can make the scattered wave pass through the field source without other interference and interaction, the problem of large oscillation caused by solving the transfer impedance is avoided. The plane wave excitation is used to simulate the complex electromagnetic field environment in the practical application of the shielded cable so that the solution of the transfer impedance is more accurate. Therefore, in this paper, a plane wave is used as the excitation source for the shielding effectiveness analysis. The plane wave equation is:

$$E_{inc} = E_0 e^{-jk_0(k-r)} \tag{1}$$

In the formula, E_{inc} is the incident wave, and E_0 is the electric field polarization vector, k_0 is the wave number in the free space, k is the propagation vector, and r is the direction vector.

The valid condition of Maxwell's equations is to assume that the field vector is single-valued, bounded, and continuously distributed in space along the direction of its derivative. Therefore, boundary conditions must be set to determine the behavior of the field when it crosses the discontinuous boundary. The radiation boundary conditions are shown in Formula (2), which are to obtain the intensity and direction of the electric field that the surface electric field vector rotates in space by solving the curl of the tangential vector of the surface electric field.

$$(\nabla \times E)_{tan} = jk_0 E_{tan} - \frac{j}{k_0} \nabla_{tan} \times (\nabla_{tan} \times E_{tan}) + \frac{j}{k_0} \nabla_{tan} (\nabla_{tan} \cdot E_{tan}) \tag{2}$$

where E_{tan} is the tangential component of the surface electric field, k_0 is the phase constant $\omega\sqrt{\mu_0\epsilon_0}$; in free space, $\mu = \mu_0 \approx 4\pi \times 10^{-7} H/m$; $\epsilon = \epsilon_0 \approx 8.85 \times 10^{-12} F/m$; j is $\sqrt{-1}$.

The ideal electric boundary conditions and the ideal magnetic boundary conditions are, respectively shown in Formulas (3) and (4):

$$\nabla \cdot (\epsilon E) = 0 \quad \hat{n} \times E = 0 \quad \hat{n} \times \nabla \times E = 0 \quad (3)$$

$$\hat{n} \cdot E = 0 \quad (4)$$

Using the electromagnetic field numerical calculation Formulas (5)–(7), the transfer impedance value of each frequency is obtained to evaluate the shielding effectiveness of the cable [12].

$$Z_T = \frac{1}{I_0} \frac{\partial V}{\partial Z} \quad (5)$$

$$\frac{\partial V}{\partial Z} = \frac{1}{A_e} \iint_{S_e} E_z dS_e \quad (6)$$

$$I_0 = \int_l H dl \quad (7)$$

where I_0 is the current flowing through the outer surface of the shielding layer, and $\partial V/\partial Z$ is the effective voltage value between the core wire and the shielding layer per unit length. E_z is the longitudinal electric field component, S_e is the inner surface of the cable shielding layer, A_e is the area of the region where S_e is located, l is the closed curve outside the cross-section of the shielding layer, and H is the tangential component of the magnetic field vector along l .

4. Results Analysis

4.1. Verification of the Conducted Emission Model of MEDS

In this paper, the standard for CE simulation analysis of the MEDS is the international standard CISPR 25-2016 [13]. In order to verify the accuracy of the simulation model in Figure 1, the conducted voltage spectrum of the LISN port was calculated and compared with the tested results in the chamber, as is shown in Figure 7. The trend of simulation and measurement in the studied frequency band of 150 kHz~30 MHz is highly consistent, which proves the correctness of the simulation model and its modeling method. Therefore, the common-mode current extracted from the simulation model is relatively reliable as the interference source of the vehicle-radiated emission.

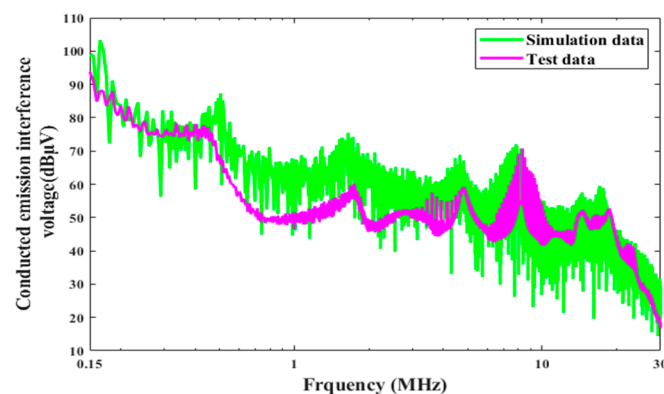


Figure 7. EMI emission simulation model of motor drive system.

4.2. Simulation Results of Shielded Cable

A comparison of the simulated transfer impedance between the shielding cable of single-layer copper braided and the shielding cable of double-layer copper braided and aluminum foil at 150 kHz~100 MHz is shown in Figure 8.

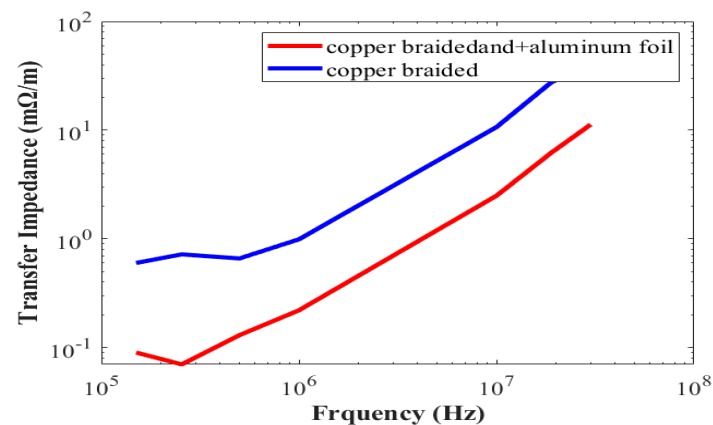


Figure 8. Impedance comparison of the two shielding modes.

As can be seen from Figure 8, compared with the transfer impedance of the single-layer copper-braided cable, the transfer impedance of the double-layer shielded cable, including copper braided and aluminum foil at 150 kHz~30 MHz, is far less, with the largest difference of 28.2 mΩ/m. According to the relationship between transfer impedance and shielding efficiency, the double-layer shielding cable provides a better shielding effect. Figure 8 shows that in order to suppress the antenna radiation effect of the cable, effective shielding should be improved. Additionally, the effects of different cable shielding can be calculated by the model in this paper.

4.3. Simulation Results of EV-Radiated Emission

4.3.1. Radiated Emission of EV without Any Suppression

In this paper, the standard for RE simulation analysis of the EV is the national standard GB/T 18387-2017 [14]. Based on the finite element method, the EMF (electromagnetic field, EMF) distribution generated in the vehicle by the electric drive and the long HVDC cable without any suppression methods and the radiated electric field were calculated, as is shown in Figure 9. According to the relationship between electromagnetic field intensity and regulatory limits, because of the high common-mode current on the HVDC cable, the radiation of the vehicle exceeds the limit in the range of 150 kHz~30 MHz.

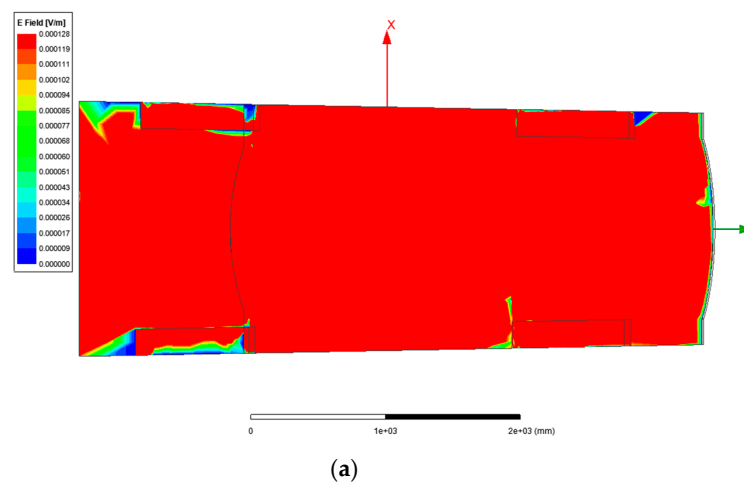
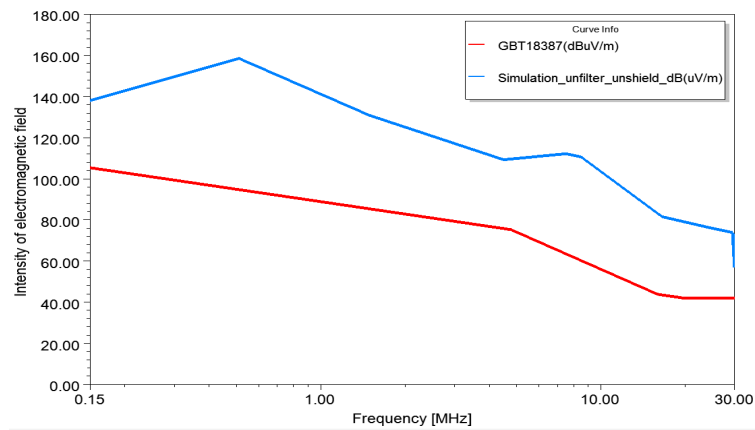


Figure 9. Cont.

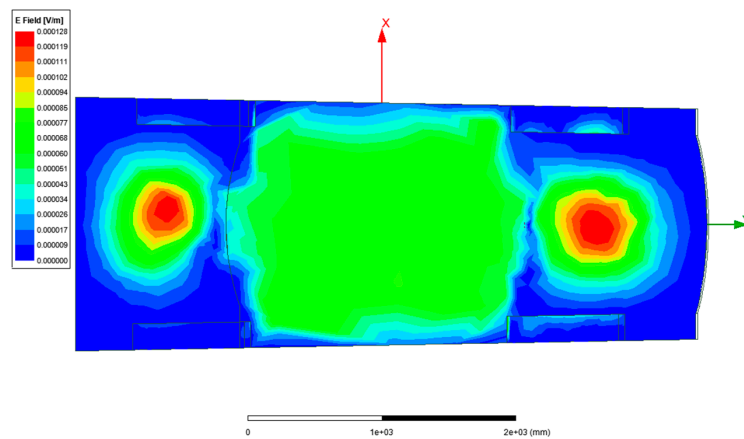


(b)

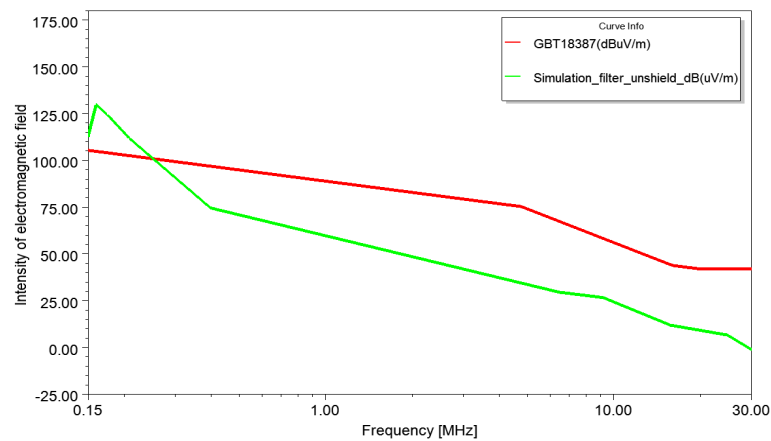
Figure 9. (a) Distribution of electromagnetic field; (b) electric field intensity at 3 m.

4.3.2. Radiated Emission of EV Using a π -Type Filter

The common-mode current on the HVDC cable with a π -type filter and the unshielded HVDC cable were imported into the vehicle for frequency domain analysis. The calculated electromagnetic field distribution and EMF emission intensity at 3 m are shown in Figure 10.



(a)



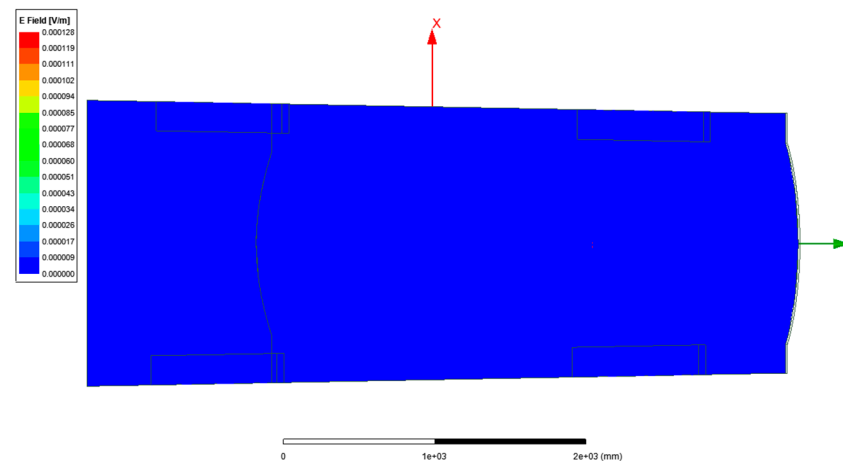
(b)

Figure 10. (a) Distribution of electromagnetic field; (b) electric field intensity at 3 m.

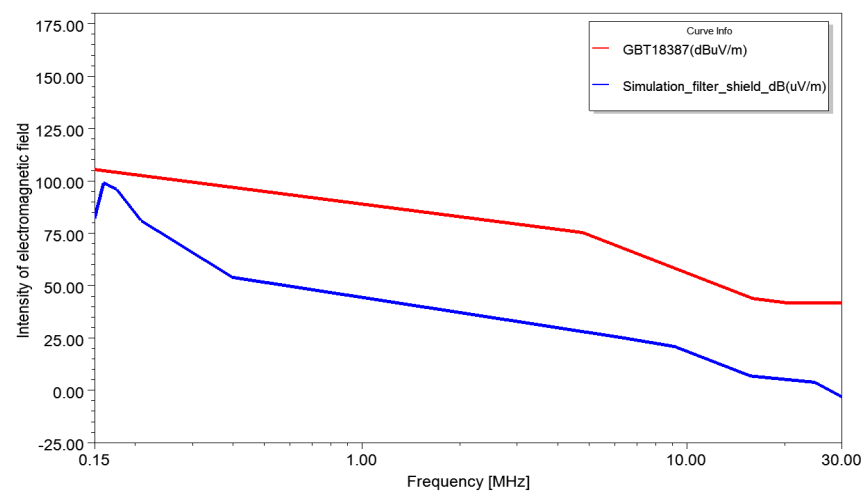
As can be seen from Figure 10, compared with the EMF intensity of the vehicle without the filter, the common-mode current and radiated emission are reduced significantly. However, the EMF still exceeds the standard at low frequency.

4.3.3. Radiated Emission of EV Using a π -Type Filter and Shielded Cables

Both a π -type filter and a double-layer shielded HVDC cable are adopted in the radiated emission model in this paper. The calculated EMF distribution is shown in Figure 11a. The relationship between the electromagnetic field and the standard limit value at a distance of 3 m from the vehicle is shown in Figure 11b.



(a)



(b)

Figure 11. (a) Distribution of electromagnetic field; (b) electric field intensity at 3 m.

When both methods are imposed, the calculated result is lower than the limit line at 150 kHz~30 MHz. It is proved that the model described in this paper can be used for risk assessment in the design stage of multi-in-one electric drive system and provide a quantitative basis for the design of interference suppression methods.

5. Conclusions

In this paper, firstly, the conducted emission model of MEDS was established, and the accuracy of the model was verified. The common-mode current on the HVDC cable was extracted based on the model, which was used as the interference source of radiated emission; the shielded cable model of HVDC cable was established, and the shielding efficiency

relationship between the single-layer shielding cable composed of copper-braided mesh and the double-layer shielding cable composed of copper-braided mesh and aluminum foil was analyzed; the radiated emission generated by the MEDS and its HVDC cable was analyzed in the EV. Finally, two typical interference suppression methods, filtering and shielding, were adopted to solve the problem in that the radiated emission exceeds the limit. The results show that different suppression methods have different effects on the radiated emission suppression. It is proved that the model described in this paper can be used for risk assessment in the design stage of MEDS and provide a quantitative basis for the design of interference suppression methods.

The innovation points of this paper mainly include the following aspects: firstly, an accurate conducted emission model of MEDS was established, which was extracted as the vehicle-radiated emission interference source; secondly, the shielding characteristics of HVDC cable was studied, which was used as the main propagation path of radiated emission; finally, a full simulation platform for EV-radiated emission which integrates interference source, interference propagation path, and interference suppression methods was established.

Nevertheless, there are some limitations of this study: in this paper, only the influence of the high-voltage system on the vehicle-radiated emission was considered; the influence of other components and the interference coupling effect between the high-voltage and low-voltage systems were not considered. Therefore, the test data of the vehicle only containing the electric drive system were difficult to obtain, and the simulation results of the vehicle-radiated emission were not verified.

The authors' next research work will include the crosstalk coupling analysis of high- and low-voltage systems and the radiated emission risk prediction analysis of the vehicle-level multi-source interference, so as to realize the highly reliable vehicle-level radiated emission risk prediction technology.

Author Contributions: Conceptualization, R.T. and S.Y.; methodology, R.T.; software, R.T.; validation, S.Y., C.Y. and C.D.; formal analysis, R.T.; investigation, C.D.; resources, A.Z.; data curation, S.Y.; writing—original draft preparation, R.T.; writing—review and editing, R.T. and S.Y.; visualization, C.Y.; supervision, A.Z.; project administration, C.Y.; funding acquisition, S.Y. All authors have read and agreed to the published version of the manuscript.

Funding: This research was funded by the National Foundation of China, grant number 2020YFB1506004.

Institutional Review Board Statement: Not applicable.

Informed Consent Statement: Not applicable.

Data Availability Statement: Not applicable.

Acknowledgments: We would like to thank editors and reviewers very much for their valuable comments in improving this article.

Conflicts of Interest: All authors are employees of Chongqing Changan New Energy Automobile Technology Co., Ltd. The paper reflects the views of the scientists, and not the company.

References

1. Jiao, J.L.; Wang, C.; Liu, Y. Simulation technology for cable harness EMC analysis. *J. Microw.* **2012**, *28*, 57–60.
2. Kreisch, K.; Kubitzek, S.; Hofmeister, C.; Barenfanger, J.; Schugt, M. Transfer Impedance Measurements and Simulations on perforated Fully-Rigid Coaxial Cables with the Line Injection and the Traxial Method. In Proceedings of the 2014 International Symposium on Electromagnetic Compatibility (EMC Europe 2014), Gothenburg, Sweden, 1–4 September 2014.
3. Zhang, J.; Wang, H.; Cai, H. Research on EMC Simulation of Electric Vehicle Drive System. *Automot. Eng.* **2014**, *36*, 580–585.
4. Zheng, L.; Long, H. Summary of EMC Research on Electric Vehicle Motor Drive System. *Chin. J. Automot. Eng.* **2014**, *4*, 319–327.
5. Xue, J. Simulation and Test of Electromagnetic Radiation inside a Pure Electric Vehicle. Master's Thesis, Chang'an University, Xi'an, China, 2018.
6. Yang, P. Research on Calculation and Measurement Method of Shielded Cable Transfer Impedance in Power System. Master's Thesis, North China Electric Power University, Hebei, China, 2005; pp. 1–4.

7. Tyni, M. Transfer Impedance of Coaxial Cables with Braided Outer Conductor. In Proceedings of the Digest of the 10th International Wroclaw Symposium on EMC, Wroclaw, Poland, 22–24 September 1976; pp. 410–419.
8. Kley, T. Optimized single-braided cable shields. *IEEE Trans. Electromagn. Compat.* **1993**, *35*, 57–63. [[CrossRef](#)]
9. Demoulin, B. Shielding Effectiveness of Braids with High Optical Coverage. In Proceedings of the International Symposium on EMC, Zurich, Switzerland, 10–12 March 1981; pp. 491–495.
10. Sali, S. A Improved Model for the Transfer Impedance Calculations of Braided Coaxial Cables. *IEEE Trans. Electromagn. Compat.* **1991**, *33*, 139–143. [[CrossRef](#)]
11. Tan, R.; Ye, S.; Deng, C.; Yu, C.; Zhou, A.; Du, C. Research on Prediction Modeling of EMI in Multi-in-one Electric Drive System. In Proceedings of the 2021 4th International Conference on Energy, Electrical and Power Engineering (CEEPE), Chongqing, China, 23–25 April 2021; pp. 621–626. [[CrossRef](#)]
12. Wang, X. Research on the Measurement and Simulation Method for Transfer Impedance of Shield Coaxial Cables. Master's Thesis, Harbin Institute of Technology, Harbin, China, 2012.
13. CISPR 25:2016. Vehicles, Boats and Internal Combustion Engines—Radio Disturbance Characteristics—Limits and Methods of Measurement for the Protection of On-Board Receivers. Available online: <http://www.iec.ch> (accessed on 30 June 2019).
14. GB/T 18387:2017. Limits and Test Method of Magnetic and Electric Field Strength from Electric Vehicles. Available online: <http://std.samr.gov.cn/gb/search/gbDetailed?id=71F772D81854D3A7E05397BE0A0AB82A> (accessed on 30 June 2019).